Some Properties of Aqueous Xanthan Gels Formed under the Action of Aluminium(III) Ions

Andrew B. Rodd[1], *Dave E. Dustan*[1], *David V. Boger*[1], *Juergen Schmidt*[2], *Walther Burchard**[2]

[1] Department of Chemical Engineering, University of Melbourne, Melbourne, Australia
[2] Institute of Macromolecular Chemistry, University of Freiburg, 79104 Freiburg, Germany

SUMMARY: Aqueous xanthan solutions form gels when aluminium salts are added and the solutions are heated above 45 °C. The gelation process was followed by dynamic light scattering. Characterization was based on the heterodyne and nonergodic approaches. Both techniques gave the same fast relaxation times, but for the slow motion much larger values were found in the heterodyne than in the nonergodic approach. The heterodyne fraction 1-*X* was found to correlate closely with the plateau height of the time correlation function (TCF) at large delay times in the nonergodic experiments. Three methods of gel point determination are demonstrated: (i) onset of heterodyne/nonergodic behavior, (ii) observation of a sharp maximum for the fast relaxation time at the gel point, (iii) observation of power-law behavior of the TCF. The statistics of nonergodic fluctuations were examined and evaluated. The potential of this procedure for detailed structure evaluation of inhomogeneities in the gel is emphasized.

Introduction

Gels are polymer networks, highly swollen in suitable good solvents. Most theories developed so far consider these systems as homogeneous in crosslinking density. However, in common crosslinking reactions such homogeneity can never be realized because once a crosslink has been formed, the local density of reactive monomer units becomes considerably larger than the overall concentration averaged over the whole system. As a consequence, the reaction around such crosslinks is favored and may also cause extensive intramolecular reaction around this domain.

Such heterogeneities can be detected by static light scattering[1,2] or by SANS and SAXS techniques, but far more efficiently by dynamic light scattering. The technique for detecting these phenomena has a long history starting probably in 1987 with Sellen[3] and reaching at present a state of two partially competing conceptions which are the *heterodyne* and the

 CCC 1022-1360/00/$ 17,50+.50/0

nonergodic approaches, associated with the names of Erik Geissler[4] and Peter Pusey[5] and his group. They may be considered as representatives of polymer and colloid sciences, respectively. The polymer scientist has to deal with flexibility and segmental mobility in a macromolecule in addition to the translational motion of the center of gravity and naturally is interested in the mobile part of a network. Pusey, on the other hand, studied glass transition and crystallization of hard colloidal particles which possess no internal mobility. He wondered how much of the material may be frozen-in so that no translational motion remained possible and was strongly interested in the immobilized fraction of the material.

Both scientists started with the same assumption that the inhomogeneous domains are drastically impeded in their mobility and can be, in a first approximation, considered as fully frozen-in. The scattering from such a system then can be treated as arising from mobile and immobilized scattering centers and can be written as

$$i(q,t) = i_F(q,t) + i_C(q) \tag{1}$$

where the subscripts F and C indicate the fluctuating and constant, i.e., frozen-in parts. Depending on whether time or ensemble averages are considered, this assumption gives rise to a derivation of the following field - time correlation functions (TCF)

$$g_H(q,t) = 1 + \frac{1}{X}[(g_2^T(q,t) - (g_2^T(q,0) - 1))^{1/2} - 1] \tag{2}$$

$$g_E(q,t) = 1 + \frac{1}{Y}[(g_2^E(q,t) - (g_2^E(q,0) - 1))^{1/2} - 1] \tag{3}$$

where $g_2(q,t)$ denotes the intensity TCF and the subscripts H and E refer to the heterodyne (H) and non-ergodic (E) approaches. These equations look mathematically equivalent. One has to look rather carefully at these equations to recognize the differences. They include on the one hand the superscripts T and E which denote time and ensemble averages and, on the other, the parameters X and Y which are given by

$$X = \frac{< i_F(q) >_T}{< i(q) >_T} \tag{4}$$

$$Y = \frac{< i(q) >_E}{< i(q) >_T} = \frac{< i_F(q) + i_C(q) >_E}{< i(q) >_T} \tag{5}$$

The fluctuating intensity is always ergodic, i.e., time and ensemble averages are the same. Hence the difference between X and Y consists in the fact that in Y the frozen-in part of the scattering intensity, which varies in different spatial positions, is incorporated in the ensemble

average, whereas in X the time average at one special cell position is taken. Clearly, the two equations become identical when $i_C(q) = 0$, i.e., for systems without immobilized domains. Actually, Eqs (5) and (6) relate to two different types of experiments: In the *heterodyne* experiment the intensity TCF is measured at one position of the scattering cell over a fairly long delay time and finally it is normalized by the time-average scattering intensity at infinitely long delay times.

In the *nonergodic* experiment the intensity TCFs are measured for a large number of different positions and the ensemble average is formed which is then normalized by the ensemble average of the static light scattering. This procedure is time-consuming.

Pusey noticed that often it is sufficient to carry out the measurement at only one position and to perform the ensemble average of the total scattering intensity at the end of these measurements by collecting the scattering intensity from a rotating cell. Nonetheless, we decided to carry out the dynamic measurements at 100 and sometimes at 500 different positions. This was possible by a special step motor that was driven by a computer program to make a rotational step of 3° when the one measurement was finished and the next run was started. To the best of our knowledge, no direct comparison of the two techniques has yet been performed with the same gel. As will be shown later, our more laborious decision proved to be appropriate.

Demonstration of two types of experiment on the time correlation functions

We applied both techniques to an aqueous xanthan solution to which $Al_2(SO_4)_3$ was added[6]. Xanthan is a microbial polysaccharide with a cellulose backbone in which every other glucose unit carries a trisaccharide as a side chain. This side chain contains one glucuronic acid unit and at the chain end a pyruvate group. Thus xanthan is a polyelectrolyte of a fairly low charge density. The chemical formula of its repeating unit is shown below.

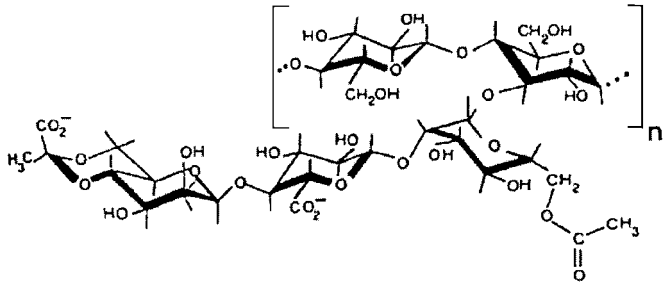

Xanthan easily forms a double-stranded helix and has a high tendency to aggregation, but it does not form gels by itself. However, when a trivalent metal salt is added, gelation can occur by electrolyte complex formation. In the present study aluminium sulfate was used as gel promoter. The actual structure of the complex is not yet known and remains as an issue to be solved by inorganic chemists using crystalline compounds of well defined oligosaccharides. The complex is not formed at low temperatures, and $Al_2(SO_4)_3$ could be added at 15 °C without causing a significant change in solution properties[6].

A technical xanthan was used. Because of remarkable chain stiffness due to the double-helix conformation, xanthan forms rather compact aggregates by side-by-side alignment. Static light scattering of untreated xanthan gave a molar mass of $M_w = 1.4\times10^9$ g/mol which corresponds to about 600 chains aggregated into one cluster. After a heat treatment at 130 °C for 30 min, a decrease in the molar mass to $M_w = 79\times10^6$ g/mol was obtained. The analysis of the scattering curve on the basis of a Casassa-Holtzer plot[7,8] permitted the determination of the linear mass density from which a lateral alignment of 16 double strands on average and a total aggregation of 34 double strands were obtained[6].

These two types of dynamic light scattering experiments led to strikingly different curves. In the *heterodyne* experiment the intercept at zero delay time decreased from the theoretical value of $g_2^T(q,0) = 2$ to a lower value and decayed for sufficiently long delay times in most cases to the base line of unity. In the *nonergodic* experiment the TCF always started at $g_2^T(q,0) = 2$ but apparently approached a plateau value of $g_2^E(q,\infty) > 1$. The following two graphs demonstrate the observations.

Heterodyne registration In Fig. 1, a number of time correlation functions from xanthan solutions containing a certain amount of Al(III) salts is shown which demonstrates the mentioned decrease in the intercept when the temperature was increased beyond 44 °C. From the intercept the magnitude of X (homodyne fraction) or 1-X (heterodyne fraction) can be calculated from the equation

$$X = 1 - \sqrt{2 - g_2^T(q,0)} \qquad (6)$$

Nonergodic registration This result is contrasted in Fig. 2 with the TCFs from the same aqueous xanthan solution. The upper part shows the intensity TCF and the lower the field TCF. As already mentioned, all curves start at the value of 2, or 1, respectively, but only for temperatures up to about 45 °C a complete relaxation to the theoretical base line was

obtained. At higher temperatures the curves no longer fully decay but seem to reach a finite plateau, whose height is easily determined. The magnitude of parameter Y requires a fit of the TCF.

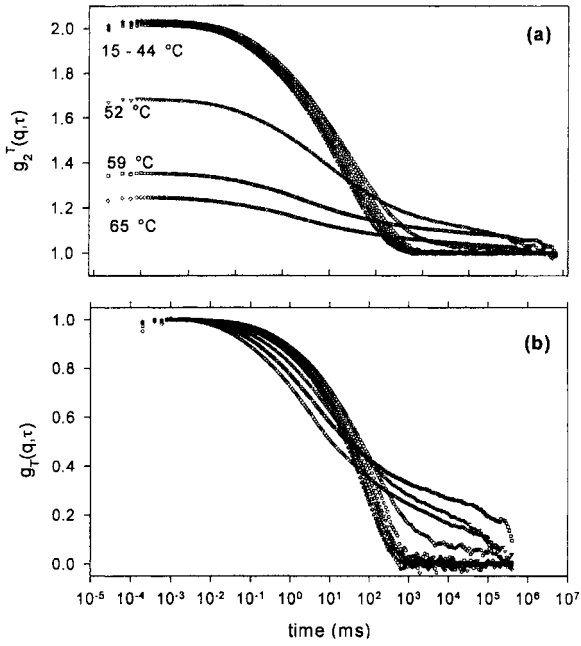

Fig. 1: *Heterodyne experiment:* (a) intensity $g_2^{\mathrm{T}}(q,t)$ and (b) field $g_{\mathrm{T}}(q,t)$ time correlation functions for 1.0 mg/mL xanthan and 2.8 mg/mL Al(III) ions in water for a range of temperatures. Conditions: argon ion laser (λ_0 = 488 nm) equipped with a pinhole, collection time 40 min before gelation, T < 45 °C and 2 h in the gel region, T > 45 °C, 30 min thermal equilibration between temperatures.

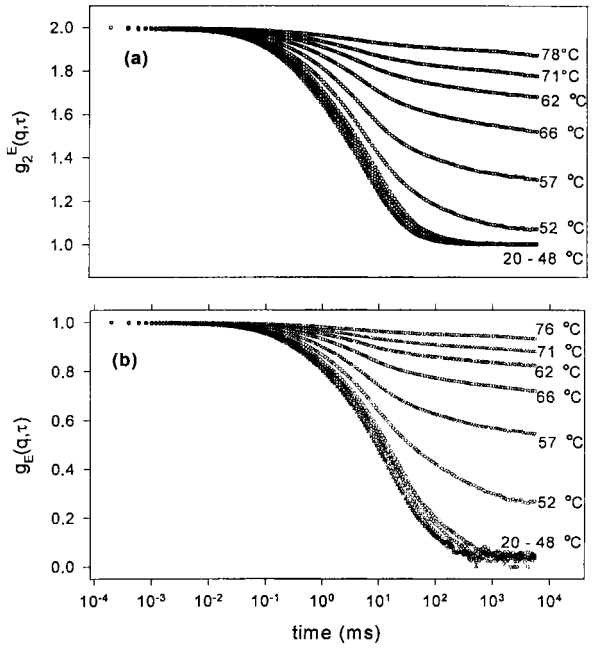

Fig. 2: *Nonergodic experiment:* (a) intensity $g_2^{\mathrm{E}}(q,t)$ and (b) field $g_{\mathrm{E}}(q,t)$ time correlation functions for 1.0 mg/mL xanthan and 2.8 mg/mL Al(III) ions in water for a temperature range. Conditions: krypton ion laser (λ_0 = 647 nm) with monomode fiber optics, 100 sample rotations with a collection time of 40 s per rotation and 30 min thermal equilibration between temperatures.

Gel point

The observation of nonergodic behavior, i.e., deviation of the ensemble average from the time average, coincided with typical gel behavior. No flow was observed when tilting the cell containing the sample. This behavior was obtained when heating the solution above 44-48 °C. The gel did not dissolve again when the sample was cooled back to room temperature. This qualitative observation could be made more precise in two ways. In one case the heterodyne fraction 1-X was plotted against the temperature and for the nonergodic experiment the plateau height was chosen. The value of X could be determined from the intercept in the intensity TCF of the heterodyne experiments as given by Eq. (6). For the other procedure, the fit of the time correlation functions with suitable model functions had to be performed.

Figure 3 shows a plot of the 1-X values against the temperature and the same for the plateau height in the nonergodic experiment. Let us take the midpoint of the two transitions as the point of gelation. Then, according to the heterodyne data, the gel point occurs close to 46 °C and, according to the nonergodic approach, at about 48 °C. Both data lie in the range of experimental errors. If the onset temperature of heterodyne or nonergodic behavior is taken as characteristics for the gel point, then the temperature would be between 43 and 44 °C.

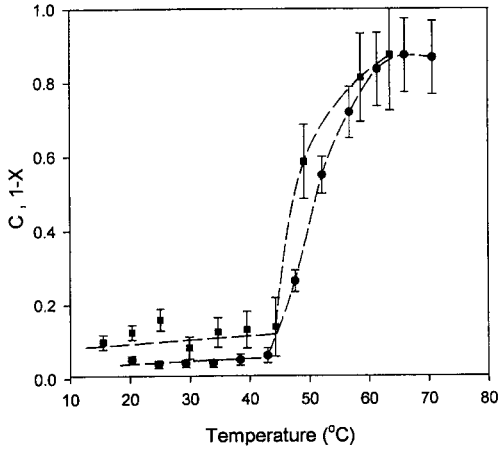

Fig. 3: Plot of the heterodyne fraction 1-X (squares) and the nonergodic plateau height (circles) as a function of temperature.

Concerning the second procedure for quantitative estimation of the gel point, we used the fit of the field TCFs with stretched exponentials. In the *nonergodic* experiment, the field TCF was fitted by two stretched exponentials[9,10,11] plus an additive constant C which described the plateau height $g_E(q, t \to \infty)$

$$g_1^E(t) = A\exp[-(t/\tau_1)^{\beta_1}] + B\exp[-(t/\tau_2)^{\beta_2}] + C \qquad (7)$$

where subscripts 1 and 2 indicate the two components, τ is the relaxation time and the value of $\beta \leq 1$ is a measure for the width of the relaxation spectrum. Both relaxations were q^2-dependent and are therefore diffusive. The diffusion coefficients are given by Eq. 8[12]

$$D_{1,2} = \frac{1}{<\tau_{1,2}> q^2} \tag{8}$$

with the mean relaxation times[11]

$$<\tau_{1,2}> = \frac{\tau_{1,2}}{\beta_{1,2}} \Gamma(1/\beta_{1,2}) \tag{9}$$

and $\Gamma(x)$ being the gamma function.

In the *heterodyne* approach, first the value of X given by Eq. (6) has to be determined and then introduced into Eq. (2) to obtain the field TCF, $g_T(q,t)$ This could be described by a relationship similar to Eq. (7) but without the constant term

$$g_1^T(t) = A\exp[-(t/\tau_1)^{\beta_1}] + B\exp[-(t/\tau_2)^{\beta_2}] \tag{10}$$

The relaxation times and the stretched exponents may not be the same as in the nonergodic approach. The fast and slow relaxations will now be considered separately.

The time dependence of the relaxation times of the fast motion is shown in Fig. 4. Remarkably, almost identical behavior was found in both approaches. Strikingly a maximum occurred near the temperature $T = 42$ °C. These findings are important and make clear that in both experiments the same fast relaxation times are registered.

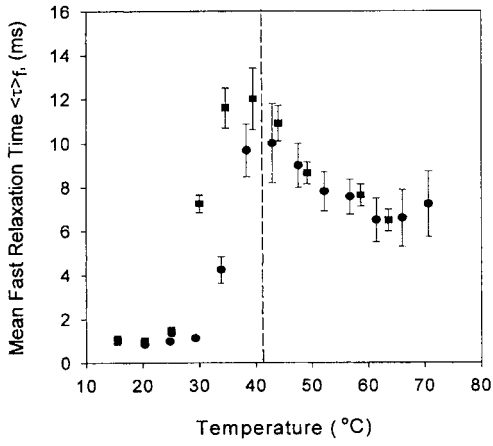

Fig. 4: Mean fast relaxation times (at 90°) from heterodyne (squares) and nonergodic (circles) experiments. The vertical line indicates the gel point.

The occurrence of the maximum can be interpreted as follows. There is much evidence that the fast motion in the pregel state arise from individual chains which become crosslinked at random via, say, point-like bonds. The clusters grow in size with progressing crosslinking as the temperature increases. Eventually, at the gel point, the sizes span the whole space of the light scattering cell, the translational motion of the center of gravity goes to zero and the relaxation time should go to infinity. Once the gel point is passed, dynamic light scattering now probes the mesh size[13] of the formed network, which becomes narrower with progressing crosslinking, and the correlation time decreases again. However, at the gel point the relaxation time actually never goes to infinity, because the network chains are at least semiflexible and the internal modes of motion still remain even when the translational motion of the center of gravity has completely stopped. Similar behavior to that shown in Fig. 4 was observed also with other gelling[14,15] samples. Thus the maximum in the relaxation time can be taken as the gel temperature, which narrows this temperature together with the data from Fig. 4 to $T_{\text{gel point}}$ = 42-44 °C if the onset of heterodyne behavior is taken as the gel point. Another criterion for the gel point followed the suggestion of Martin and Wilcoxon[16], and a theoretical prediction by Muthukumar who claimed power-law behavior of the TCF at the gel point with an exponent n which is determined by the fractal dimension d_f of clusters near the gel point as[17]

$$d_f = \frac{7.5 - 3n}{3 - n} \tag{11}$$

We found such power-law behavior with an exponent $n = 0.63 \pm 0.01$ with a fractal dimension of $d_f = 2.37 \pm 0.06$ which is typical of branched clusters[18-20].

Next the slow motion may be considered. Figure 5 shows the result from the two types of experiments.

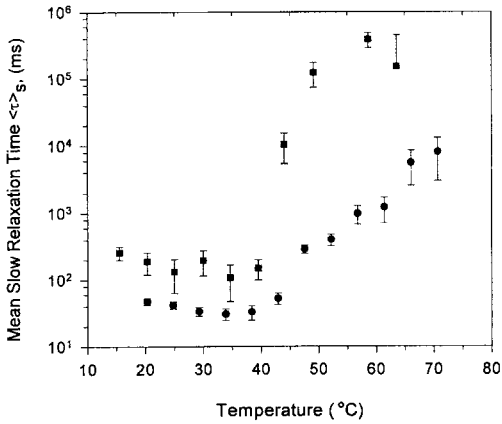

Fig. 5: Mean slow relaxation times as a function of temperature as registered in the heterodyne experiment (squares) and the nonergodic experiment (circles). Note the logarithmic scale in comparison with the linear scale in Fig. 4.

Now the relaxation times determined by the heterodyne approach increase much stronger with temperature and the values are up to 150 times larger than those observed in the nonergodic experiment. The explanation for this stunning discrepancy follows from the initial conditions of the two experiments. The nonergodic experiment was time-consuming because the intensity TCF was measured at 100 different positions and, in the end, the ensemble average was taken. Therefore, the range of delay times had to be truncated. In the present case to 40 s which added up to 1000 s for measurement at one scattering angle. In the heterodyne experiment the longest delay time was 45 min = 2700 s, i.e., about 70 times longer[6]. Thus everything that moves more slowly than 40 seconds is considered in the nonergodic experiment as an immobile rock. This limit was shifted in the heterodyne experiment to 2700 s and what appeared to be a rock was actually still slowly moving. Similar observations were recently made by Cipelletti et al.[21] in small-angle dynamic light scattering from a glassy colloidal material, and even here he found a complete decay to the baseline with a correlation time of about 24 h.

At this point the question arises: what may be the origin of the slow motion ? In xanthan a slow motion is present already at low temperatures without added aluminium salt and causes a huge molar mass of about 1.4×10^9 g/mol with a radius of gyration[6] R_g = 409 nm. This corresponds to an aggregate of about 600 xanthan chains, partly side-by-side-aligned (molar mass of a double-helix (DH) xanthan $M_{w,DH} = 3.5\times10^6$ g/mol [22-25]). Upon a 30-min heat treatment at 130 °C the molar mass was reduced to 79×10^6 g/mol and a radius of gyration of R_g = 315 nm, i.e. corresponding to aggregates (about 16) of about 34 now mainly laterally aligned chains. The aggregates remain present during the crosslinking reaction and apparently grow in size. These rather compact aggregates differ from speckles, which give rise to the nonergodic fluctuations.

Statistics of speckles and evaluation of the fluctuating and constant contributions

The next question to be answered is what the actual size and structure of these heterogeneities may be. This question is a rather involved problem which has not yet been fully solved. We followed a suggestion by Joosten and Pusey[26] and evaluated the spatial fluctuation by a statistical treatment. Like Joosten et al., who studied polyacrylamide gels, we registered the scattering intensity from the xanthan gel at 57 °C at 520 positions time-averaged over 40 s. The result is shown in Fig. 6.

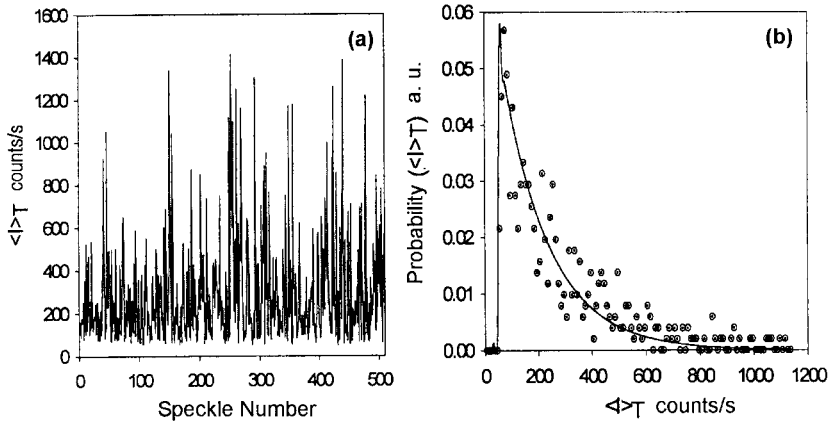

Fig. 6: (a) Scattering intensities at 520 different cell positions averaged over 40 s. Measurements were made with the xanthan gel at 57 °C. (b) Histogram of the peak distribution in (a). The full line corresponds to Eq. (12) derived by Pusey[5,27]

$$P(< I(q) >_T) \propto H(< I(q) >_T) - < (I(q) >_F \exp\left[- \frac{< I(q) >_T - < I(q) >_F}{< I(q) >_E - < I(q) >_F} \right] \quad (12)$$

In Fig. 6a one notices a fairly constant minimum scattering intensity upon which a strong scatter in the intensity is superimposed. Evidently the constant part represents the fluid term for which the time average equals the ensemble average and the strongly fluctuating peaks relate to the speckles where the peak height is the product of the molar mass of the non-moving particle times the partial concentration of the non-moving heterogeneities. Hence the peak height may correspond to very large domains with a low concentration in the detection volume or it can arise from many but much smaller immobilized domains. Statistical techniques can be applied to get information on the size distribution of these heterogeneities which is shown in Fig. 6b. This distribution could be described[5,27] by Eq. (12) which allowed to extract the desired information on the average size times the amount of immobile domains, which is an ensemble average, and on the contribution of the ergodic scattering intensity. For the xanthan gel, the ratio $<i_F(q)>_T/<i_C(q)>_E = 0.2$ was obtained[6] at 90°, whereas Joosten[26] obtained for the acrylamide gel at 150° $<i_F(q)>_T/<i_C(q)>_E = 0.6$. Apparently the polyacrylamide gel contained less rock-like heterogeneities than the xanthan gel.

Angular dependence

Both the fluid part and the large heterogeneities will have a different angular dependence. Measurement of these two components as a function of the scattering angle will provide us with detailed information on the structure of the two components separately. Panyukov and Rabin[28] tried to set up a basic theory of this angular dependence. Their theory is basically an extension of the well-known Tanaka[29] theory of networks who neglected the existence of immobile heterogeneities. The theory is complex and resulted in an angular dependence which is difficult to interpret in physical terms. Their result does not appear to be in agreement with preliminary observations. Probably the theory could be considerably simplified when starting with reasonable assumptions on the structure of the two components. Although the study of the angular dependence will be considerably time-consuming, the invested effort will be worthwhile because, in addition to the information on size and structure, the distribution of sizes of the heterogeneities would be possibly accessible to determination.

Conclusions

Two main results can be obtained from this comparison of the heterodyne and nonergodic experiment: (i) The fast motion is correctly determined in both experiments. It represents the fluid part in a gel which is ergodic and the time and ensemble averages coincide. (ii) The value of the heterodyne fraction $1\text{-}X = 1 - \langle i_F(q)\rangle_T/\langle i(q)\rangle_T$ correlates strongly with the asymptotic plateau height in the nonergodic experiment. Furthermore, dynamic light scattering allows to determine the point of gelation in several ways, among others by the onset of heterodyne or nonergodic behavior, by the maximum of the correlation time corresponding to translational diffusion and by checking when the power-law behavior of the TCF is observed.

It does not seem to make any serious difference which type of experiment is chosen as long as the heterodyne experiment is conducted to very long delay times. The heterodyne experiment is easier carried out and is less time-consuming, but it can no longer be satisfactorily applied in detectors equipped with the monomode fiber optics. Only with pinhole optics we could register a sensibly smooth heterodyne signal. If monomode fiber optics is used, one obtains either a heterodyne signal or just a homodyne response. The reason for this becomes clear from Fig. 7 which shows the time dependence of the scattered light at one cell position. With monomode-fiber optics only a tiny scattering volume is probed. Thus in one case only the

liquid ergodic fraction is registered, in another only a speckle. Thus sensible nonergodic observations at one position can be made when either a sufficient number of speckles is present in the detection volume or the detection volume has to be increased to the size of the scattering volume if possible. This was achieved with the pinhole setup. This statement holds true for *pseudo*-nonergodic systems which eventually become ergodic at sufficiently long delay times.

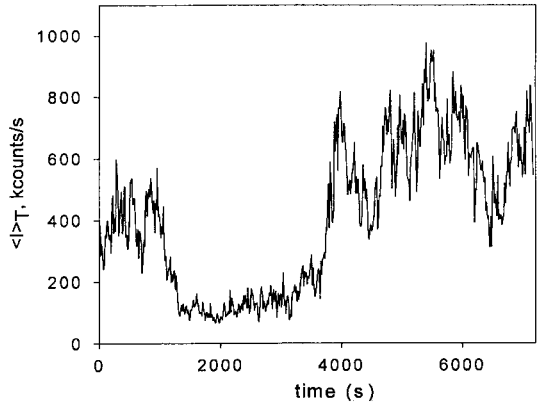

Fig. 7: Change of the scattering intensity from xanthan gel with time observed with monomode fiber optics (57 °C). Each value was time-averaged over 40 s. Note the time scale in the beginning when one speckle is registered. After 1500 s = 25 min, the speckle moved out of the volume of observation, and approximately after 30 min only the ergodic fluid part is registered, until another, bigger speckle entered the observation volume.

References

1. T. Coviello, W. Burchard, E. Geissler, D. Maier, *Macromolecules* **30**, 2008 (1997)
2. W. Burchard, *Biomacromolecules* **2**, 342 (2001)
3. D. B Sellen, *J. Polym. Sci. B: Polym. Phys.* **25**, 699 (1987)
4. E. Geissler, *Dynamic Light Scattering from Gels*, in: *Dynamic Light Scattering*, W. Brown (Ed), Clarendon Press, Oxford 1993, Chap. 13
5. P. N. Pusey, W. van Megen, *Physica A* **157**, 705 (1998)
6. A. B. Rodd, D. E. Dunstan, D. V. Boger, J. Schmidt, W. Burchard, *Macromolecules* **34**, 3339 (2001)
7. E. F. Casassa, *J. Chem.Phys.* **23**, 596 (1952)
8. A. Holtzer, *J. Polym. Sci.* **17**, 432 (1952)
9. R. Kohlrausch, *Poggendorff Anal. Chem.* **91**, 179 (1854); **119**, 337 (1863)
10. G. Williams, D. C. Watts, (a) *Trans. Faraday Soc.* **66**, 80 (1970); (b) G. Williams, D. C. Watts, A. M. Worth, *Trans. Faraday Soc.* **67**, 1323 (1971)
11. G. D. Patterson, *Adv. Polym. Sci.* **48**, 124 (1983)
12. See books on dynamic light scattering, e.g., B. J. Berne, R. Pecora, *Dynamic Light Scattering*, Wiley, New York 1976
13. P.-G. de Gennes, *Scaling Concepts in Polymer Physics*, Cornell University Press, Ithaca, NY, 1979
14. T. Fuchs, W. Richtering, W. Burchard, K. Kajiwara, *Polym. Gels Networks* **5**, 541 (1997);

15. (a) W. Burchard, P. Lang, L. Schulz, T. Coviello, *Macromol. Symp.* **58**, 21 (1992); (b) W. Burchard, T. Aberle, T. Fuchs, W. Richtering, T. Coviello, E. Geissler, L. Schulz, *The Wiley Polymer Networks Group Review Series* **1**, 13 (1998)
16. J. E. Martin, J. Wilcoxon, *Phys. Rev. Lett.* **62**, 373 (1988)
17. (a) M. Muthucumar, *J. Chem. Phys.* **83**, 367 (1985); (b) *Macromolecules* **22**, 4656 (1989)
18. D. Stauffer, *Introduction to Percolation Theory*, Taylor & Francis, London 1985
19. M. Daoud, J. E. Martin, in: *The Fractal Approach to Heterogeneous Chemistry*, D. Avnir (Ed), Wiley, New York 1989
20. W. Burchard, *Adv. Polym. Sci.* **143**, 113 (1998)
21. L. Cipelletti, S. Manley, R. C. Ball, D. A. Weitz, *Phys. Rev. Lett.* **84**, 2275 (2000)
22. G. Holzwarth, *Carbohydr. Res.* **66**, 173 (1978)
23. M. Dentini, T. Coviello, K. Kajiwara, V. Crescenzi, W. Burchard, *Macromolecules* **21**, 312 (1982)
24. G. Berth, H. Dautzenberg, B. E, Christensen, S. E. Harding, G. Rother, O. Smidsrod, *Macromolecules* **29**, 3491 (1996)
25. I. Capron, G. Brigand, G. Muller, *Polymer* **38**, 5289 (1997)
26. J. G. H. Joosten, J. L. McCarthy, R. N. Pusey, *Macromolecules* **24**, 6690 (1991)
27. P. N. Pusey, *Macromol. Symp.* **79**, 10 (1994)
28. S. Panyukov, Y. Rabin, *Macromolecules* **29**, 7960 (1996)
29. T. Tanaka, L. O. Hocker, G. B. Benedek, *J. Chem. Phys.* **59**, 5151 (1973)